


AUTHOR QUERY FORM

	<p>Journal: J. Chem. Phys.</p> <p>Article Number: JCP19-AR-PLAS2020-04143</p>	<p>Please provide your responses and any corrections by annotating this PDF and uploading it to AIP's eProof website as detailed in the Welcome email.</p>
---	--	--

Dear Author,

Below are the queries associated with your article. Please answer all of these queries before sending the proof back to AIP.

Article checklist: In order to ensure greater accuracy, please check the following and make all necessary corrections before returning your proof.

1. Is the title of your article accurate and spelled correctly?
2. Please check affiliations including spelling, completeness, and correct linking to authors.
3. Did you remember to include acknowledgment of funding, if required, and is it accurate?

Location in article	Query/Remark: click on the Q link to navigate to the appropriate spot in the proof. There, insert your comments as a PDF annotation.
Q1	Please check that the author names are in the proper order and spelled correctly. Also, please ensure that each author's given and surnames have been correctly identified (given names are highlighted in red and surnames appear in blue).
Q2	We have reworded the sentence beginning "We analyze a..." for clarity. Please check that your meaning is preserved.
Q3	References 32, 33, and 37 were not cited in the text. We have inserted a citation in the sentence beginning "TDDFT and DFTB..." Please check our placement and reposition if necessary.
Q4	In the sentence beginning "The dependency of. . .," please confirm that "the previous section" refers to Sec. III.
Q5	In the sentence beginning "The function $F(R, L)$..." there was an extra closing bracket; therefore, we have deleted it. Please check.
Q6	In the sentence beginning "Using the parameters..." there was a missing closing parenthesis; therefore, we have inserted it. Please check.
Q7	References (34 and 38) and (41 and 49) contain identical information. Please check and provide the correct reference or delete the duplicate reference. If the duplicate is deleted, renumber the reference list as needed and update all citations in the text.
Q8	We were unable to locate a digital object identifier (doi) for Refs. 39 and 44. Please verify and correct author names and journal details (journal title, volume number, page number, and year) as needed and provide the doi. If a doi is not available, no other information is needed from you. For additional information on doi's, please select this link: http://www.doi.org/ .
Q9	Please provide publisher's name in Ref. 46.
Q10	In Ref. 47, please provide a brief description of the information available at the website. For example, "See XX for information about XXX."

Continued on next page.

Continued from previous page.

Please confirm ORCID(s) are accurate. If you wish to add an ORCID for any author that does not have one, you may do so now. For more information on ORCID, see <https://orcid.org/>.

A. S. Fedorov – 0000-0002-7911-3301

P. O. Krasnov – 0000-0002-5843-0455

M. A. Visotin –

F. N. Tomilin – 0000-0002-3578-6141

S. P. Polyutov – 0000-0003-1366-1986

H. Ågren –

Please check and confirm the Funder(s) and Grant Reference Number(s) provided with your submission:

Russian Science Foundation, Award/Contract Number 18-13-00363

Please add any additional funding sources not stated above.

Thank you for your assistance.

Author Proof

Charge-transfer plasmons with narrow conductive molecular bridges: A quantum-classical theory

Cite as: J. Chem. Phys. 151, 000000 (2019); doi: 10.1063/1.5131734

Submitted: 15 October 2019 • Accepted: 9 December 2019 •

Published Online: XX XX XXXX



A. S. Fedorov,^{1,2,3,a)} P. O. Krasnov,^{2,3,4} M. A. Visotin,^{1,3} F. N. Tomilin,^{1,3} S. P. Polyutov,^{1,3,b)} and H. Ågren^{2,5}

AFFILIATIONS

¹Kirensky Institute of Physics, Federal Research Center KSC SB RAS, 660036 Krasnoyarsk, Russia

²Federal Siberian Research Clinical Center under FMBA of Russia, 660037 Krasnoyarsk, Russia

³Siberian Federal University, 660041 Krasnoyarsk, Russia

⁴Reshetnev Siberian State University of Science and Technology, 660037 Krasnoyarsk, Russia

⁵Division of Theoretical Chemistry and Biology, Royal Institute of Technology, SE-100 44 Stockholm, Sweden

Note: This paper is part of the JCP Special Topic on Emerging Directions in Plasmonics.

^{a)}Electronic mail: alex99@iph.krasn.ru

^{b)}Electronic mail: spolyutov@sfu-kras.ru

ABSTRACT

We analyze a new type of plasmon system arising from small metal nanoparticles linked by narrow conductive molecular bridges. In contrast to the well-known charge-transfer plasmons, the bridge in these systems consists only of a narrow conductive molecule or polymer in which the electrons move in a ballistic mode, showing quantum effects. The plasmonic system is studied by an original hybrid quantum-classical model accounting for the quantum effects, with the main parameters obtained from first-principles density functional theory simulations. We have derived a general analytical expression for the modified frequency of the plasmons and have shown that its frequency lies in the near-infrared (IR) region and strongly depends on the conductivity of the molecule, on the nanoparticle–molecule interface, and on the size of the system. As illustrated, we explored the plasmons in a system consisting of two small gold nanoparticles linked by a conjugated polyacetylene molecule terminated by sulfur atoms. It is argued that applications of this novel type of plasmon may have wide ramifications in the areas of chemical sensing and IR deep tissue imaging.

Published under license by AIP Publishing. <https://doi.org/10.1063/1.5131734>

I. INTRODUCTION

Surface plasmons (SPs) are delocalized collective oscillations of free electrons relative to the positive ions at the interface between negative and positive permittivity materials, such as metal-dielectric interfaces. SPs are associated with oscillations of charge density coupled with electromagnetic fields (EMF) created by the coherent motion of the free charges. These oscillations are called surface plasmon polaritons in the case of planar interfaces or localized surface plasmons (LSPs) in the case of metal nanoparticles (NPs) with a closed surface.^{1,2} The plasmon polaritons are characterized by a specific frequency (surface resonant frequency, SRF) when the incident electromagnetic radiation is resonant with the surface plasmon

resonance (SPR) frequency. The SRF is highly sensitive to the permittivity of a surrounding chemical environment, the change of which due to chemical composition and morphology often leads to substantial shifts of the SRF.^{3–6}

Since the SRF can be readily measured by different optical techniques,³ LSPs are nowadays intensively used for the creation of nanoscale sensors for chemical and biological substances.^{4–7} Moreover, the strong local electromagnetic field enhancements offered by plasmon excitation has rendered a wide use of plasmonic materials in different fields, such as high resolution imaging,⁸ plasmon lasers,⁹ chemical synthesis,¹⁰ water splitting,¹¹ optical waveguiding,^{12–15} biomedical and telecom applications,^{16,17} and photovoltaic cells,^{1,18–21} just to name a few.

Gold is the most known substance for plasmonic applications due to its light absorption in the visible region. It is often used in the form of separate nanoparticles (NPs), nanorods or 3-D materials built from NPs.^{22,23} Besides Au NPs, silver and copper nanoparticles are also employed, albeit to a lesser extent due to their instability.^{1,4,7,8,10,19,21} A variety of different forms of plasmonic materials are conditioned by the fact that the LSP is concentrated at the edges of the nanoparticles, that the strength of the electromagnetic field strongly depends on the interaction and the interparticle distance, and that small changes are very influential on the measured signal. From this point of view, the SRF also depends on the size and shape of the nanoparticles¹⁻⁶ as well as the type of material that links them.⁵ In the case of conductive materials between two nanoparticles a new mode, called charge transfer plasmon (CTP), emerges. Such plasmons, observed in the case of conductively coupled metallic nanoparticles, are expected to expand their applications from molecular sensing to nanoscale wave-guiding.

An example of charge transfer plasmons was experimentally observed in Ref. 5 in a system consisting of two gold NPs with diameter $D \geq 40$ nm joined by a cylindrical gold bridge with radius from 10 to 20 nm. The CTP was described by classical Maxwell's electrodynamics as quantum effects were not expected to be significant due to the large system size. Quantum effects of CTPs have subsequently been investigated in systems consisting of two NPs separated by subnanometer interparticle gaps,^{5,25-27} where the coupling of the nanoparticles is conditioned by tunneling between them and by screening effects. However, CTPs have not been investigated for systems consisting of NPs connected by narrow conductive bridges (conducting organic molecules, COMs), where the importance of quantum effects is expected—this is precisely the topic of the present study. We thus consider here a hybrid model that exhibits CTPs consisting of two metallic NPs connected by a thin COM and analyze the implications of such systems, which thus are novel for plasmonic generation.

II. APPLIED APPROACHES FOR CALCULATING OF ELECTRON TRANSPORT AND PLASMON OSCILLATIONS

Generally, theoretical descriptions of plasmon resonances in bulk materials can be based on Maxwell's equations. At least, measured plasmon peak positions and spectral areas in bulk metals are found to be in good agreement with classical theory predictions. However, surface plasmon resonance widths in conductive nanostructures are significantly influenced by quantum confinement effects. Thus, in the case of small nano-objects, they cannot be reproduced using the dielectric functions of bulk materials.²⁴

The simplest bulk plasmon description can be obtained in terms of simple electrostatics and assuming that the electron is a classical particle having mass m and coordinate x as a function of time $\tilde{x}(t)$,

$$m\ddot{\tilde{x}}(t) = e\vec{E} = -4\pi ne^2\tilde{x}(t). \quad (1)$$

Such an approach, however, cannot be used for the here suggested NPs-COM systems because the nature of the restoring force

acting on the electron will be different and because a COM has a few conducting channels where electrons in the vicinity of the Fermi level E_{Fermi} will conduct current. Thus, quantum effects of free carrier motion are vital in COMs, which calls for a strict treatment by wave function time evolution $\psi(r, t)$ ³⁸ in the frame of the real-time propagation approaches, such as real-time time-dependent density functional theory (TDDFT).³⁰ Unfortunately, to avoid the errors accumulating in this technique, the chosen time step needs to be very small (~ 0.001 fs), which currently restricts the system size to ~ 250 noble (Au, Ag) atoms, while, as it was mentioned above, an observation of SPRs is possible only in the case of nanoparticles consisting of hundreds of atoms. Therefore, it is vital to develop a methodology to calculate the plasmon frequencies in NPs-COM systems where the NP size is larger than a nanometer, while at the same time, the electron current through the COM narrow bridge should be treated by a quantum-mechanical approach. The methodology should make it possible to calculate the longitudinal plasmonic frequencies in dependence of the nanoparticle diameter and also the conductive properties of the organic molecule connecting the NPs. As a first step in this methodology, it is necessary to study the electronic conductivity in the systems. The Landauer method is usually used for this purpose,⁴¹ according to which the effective current I at zero temperature between two electrodes possessing μ_1 and μ_2 electrochemical potentials, respectively, can be estimated as a difference of currents from one electrode to the other one, $I = I^+ - I^-$, where

$$I^+ = \frac{e}{L} \sum_{k,n} \frac{\partial E(k)}{\hbar \partial k} f(E, \mu_1), \quad (2)$$

$$I^- = \frac{e}{L} \sum_{k,n} \frac{\partial E(k)}{\hbar \partial k} f(E, \mu_2). \quad (3)$$

Herein, $f(E, \mu_1) = 1/(\exp[(E - \mu_1)/(k_b T)] + 1)$ is the Fermi function of one electrode with potential μ_1 and n and k are the indices of each transverse mode and wave number of electron state $\{n, k\}$ moving along the narrow bridge simultaneously.

Usually in the range $E(k) \in [\mu_1 \dots \mu_2]$, a fixed number $M(E)$ of the channel conducting electrons throughout the bridge is constant $M(E) = \sum_n f(E, \epsilon_n)$. So, applying (1) and replacing the summation over k by integration over E , the total current I can be written as

$$I = I^+ - I^- = \frac{2e^2}{h} M \frac{(\mu_1 - \mu_2)}{e} \\ \Rightarrow G = \frac{2e^2}{h} M, \quad (4)$$

where G is the system conductivity and $M = M(\mu_1) - M(\mu_2)$. If we take into account that an electron has some reflection rate during its motion from one electrode to the other at low bias, Eq. (4) would be transformed into the well-known Landauer⁴² formula, $G = (2 \times 10^2)/h * TM$, where $T = T(E)$ is the transmission coefficient at any energy $E \in [\mu_1 \dots \mu_2]$. If the bias $[\mu_1 \dots \mu_2]$ is sufficiently large so that $T(E)$ and $M(E)$ can be varied within the range, this formula can be substituted by an integral⁴³

$$\frac{e}{h} \int_{-\infty}^{+\infty} T(E) [f(E, \mu_1) - f(E, \mu_2)] dE,$$

156 which transforms at temperature $T = 0$ into

$$157 \quad \frac{e}{\hbar} \int_{\mu_2}^{\mu_1} T(E) dE.$$

158 Unfortunately, the Landauer approach in the original form is not
159 profitable for a description of the proposed plasmon model because
160 this approach does not account for the influence of the electromag-
161 netic field (EMF) on the electron acceleration during the motion
162 inside a narrow conductor. It proclaims the change of total elec-
163 tron energy instead, or, in other words, the change of electrochem-
164 ical potential in the electrode. However, a change of the electronic
165 state in the COM region due to the influence of an EMF is essen-
166 tial for the plasmon vibration description. Another reason why the
167 Landauer approach is not profitable for our model is the assumed
168 constant bias, while in the case of plasmon oscillations, the bias and
169 current are varied according to the harmonic law. In that context,
170 we note that, recently, some progress has been accomplished for AC
171 calculations inside narrow channels.^{48–50} For example, biased molec-
172 ular junctions subjected to external time-dependent electromagnetic
173 fields have been addressed by solutions of coupled Green's func-
174 tions of the quantum system and Maxwell's equations for electric
175 and magnetic fields.⁵⁰ Unfortunately, this method is too compli-
176 cated to use for real systems, due to the nature of the self-consistent
177 differential equations for Green functions for electron state calcu-
178 lations. In addition, solutions of the simultaneous Maxwell's equa-
179 tions obtained by sampling in time and space regions using the
180 finite-difference-time-domain (FDTD) approach are also expensive.
181 Due to these reasons, this method has been used for model systems
182 only, where the conductive molecule is represented by a bridge in
183 two-level systems.⁵⁰

184 In another example,⁴⁸ the equation of motion for density oper-
185 ator $\hat{\rho}(t)$, projected onto the subspace of molecular degrees of free-
186 dom, was formulated in the weak molecule-leads coupling limit,
187 where this junction has a time-periodic modulation of the chemi-
188 cal potential of the leads. For periodic time-dependent terms, the
189 charge transport kinetics were mapped onto a static problem of a
190 molecule interacting with multiple leads. The time-averaged cur-
191 rent reproduces the results of scattering approaches to transport
192 through conductance channels with time-dependent perturbations,
193 as derived using the Floquet theory.⁵¹ Unfortunately, this method is
194 also too complicated to be used for real systems and is restricted to
195 model systems only.

196 Time-dependent density functional theory (TDDFT) quantum
197 method has been successfully used for the description of quantum
198 effects related to plasmons.^{28–30} It has been shown, for example,
199 that Ag-Au nanoparticles are very sensitive to the chemical con-
200 figuration, and in some cases, the position of the atomic species
201 outweigh the effect of changing composition.³¹ Density Functional
202 based Tight Binding (DFTB) methods have been used, for example,
203 for the study of optical properties and the electronic structure of Ag
204 nanorods and nanorod dimers³⁴ and for the description of influence
205 of quantum tunneling on the efficiency of excitation energy trans-
206 fer in plasmonic Ag NPs chain waveguides.⁵⁵ TDDFT and DFTB,
207 being quantum methods, are, however, very time-consuming meth-
208 ods and the possibility of their practical use strongly depends on
209 the size of the NPs, i.e., the number of atoms and electrons.^{32,33,37}
210 Therefore, the applications are limited to the consideration of small

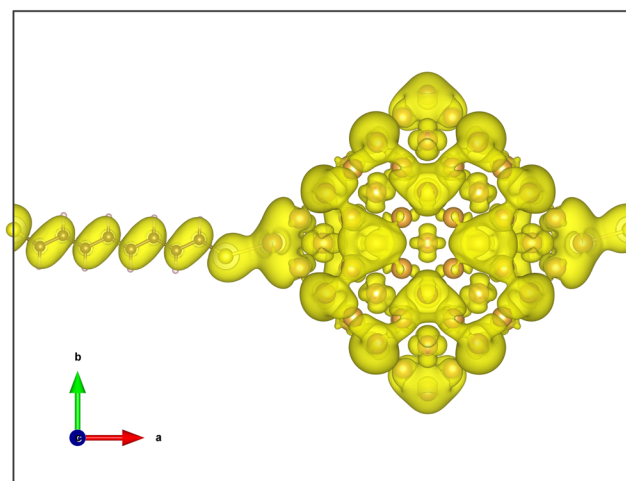
211 particles, consisting, in most cases, of a maximum of a few hundred
212 atoms.^{31,34,35}

213 III. MODELING OF CHARGE-TRANSFER IN A PAIR 214 OF METAL NANOPARTICLES BOUND 215 BY A CONDUCTING MOLECULE

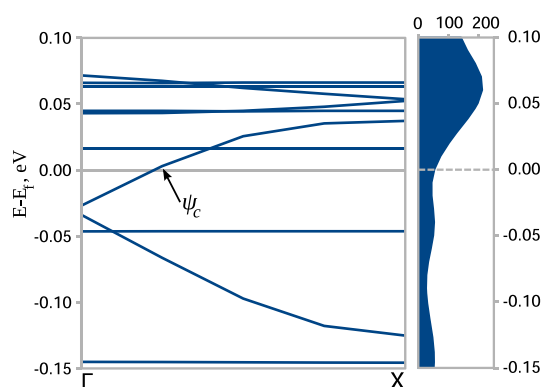
216 To construct the model, we have considered a system consisting
217 of two gold nanoparticles of 147 atoms connected by a polyacetylene
218 molecule C_8H_8 , having conjugated chemical bonds, where the junc-
219 tions with the NPs are implemented by the sulfur atoms to ensure
220 the electric conductivity of the full NP-COM-NP system. Nanoparti-
221 cles of such size exhibit metallic properties due to thermal excitation
222 [see the solid electronic density of states (DOS) near E_{Fermi} in Fig. 2]
223 where the Gaussian broadening 0.03 eV was used, which is compa-
224 rable with the thermal broadening at temperature 300 K. The NP
225 metallic properties are essential for our model, where carriers move
226 between the two nanoparticles. Herein, it must be noted that the use
227 of sulfur atoms is a well-known practice for organic linker molecules
228 to be attached to gold nanoparticles.

229 It is assumed that the conductive bridge is actually a one-
230 dimensional conductor in which electrons or holes move in a ballis-
231 tic mode, i.e., the mean free path of the carriers exceeds the length
232 of the bridge.

233 The key point of our model is the consideration of electron
234 dynamics, which is described in the language of the wave function.
235 Under the applied electrostatic field, the conduction electrons would
236 accelerate, which leads to a change in their quasimomentum \vec{k}
237 and the band energy $E(\vec{k})$. Changes in these quantities can easily be cal-
238 culated from the knowledge of only the band structure and effective
239 electron mass m^* near E_{Fermi} . On the basis of so-called effective mass
240 theorem, equation $\hbar \vec{k} = \vec{p} = e\vec{E}$ is proved,³⁶ which is basic when
241 considering the dynamics of an electron and establishing the exact
242 relationship between quantum and classical quantities—a quasimo-
243 mentum, momentum, and external force. Therefore, the method



244 FIG. 1. Geometry and electron density of the conductive band for $k \cong k_f$ of the
245 periodic $[-Au_{147}-S-C_8H_8-S]-$ system.

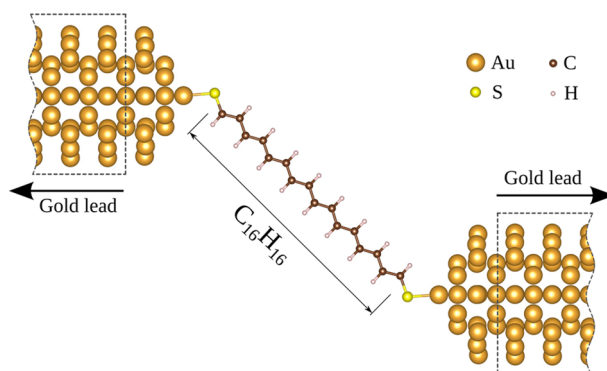


246 **FIG. 2.** Band structure (left) and DOS (right) of periodic $[\text{Au}_{147}\text{-S-C}_8\text{H}_8\text{-S}]$ system. The Fermi level is set to 0. Symbol Ψ_c denotes the position of the electronic state in the conductive band, for which the electron density is shown in Fig. 1.

249 that uses the exact relationship between quantum and classical quantities is significantly easier compared to known methods based on nonequilibrium quantum Green functions⁵⁰ or quantum real-time propagation of wave functions in the frame of time-dependent density functional theory (real-time TDDFT) approaches.²⁸⁻³⁰ These methods can only be used for sufficiently small systems or model systems. An important assumption of the proposed model is also that the conductivity of nonperiodical NP-COM-NP systems is similar to that of the corresponding periodic (NP-COM) systems.

259 This assumption can be justified by the fact that the local dynamics of an electron inside the COM between two NPs is determined by the local electric field and does not depend strongly on the contacts of these NPs with other COMs in periodic systems. This allows us to simplify the calculations of the electron dynamics in NP-COM-NP systems and calculate the effective electron mass near E_{Fermi} only in the corresponding periodical system.

267 In this work, calculations of the system geometry, electronic properties, and band structure were carried out within density functional theory with gradient decomposition (DFT-GGA), using the VASP 5.4 software.^{39,40} The results of these calculations indicate



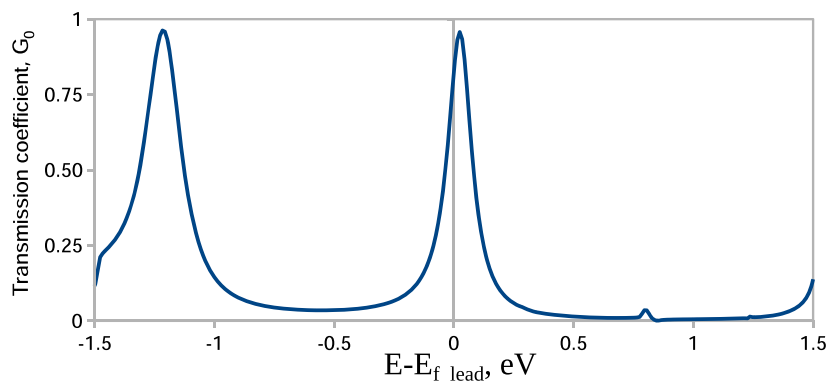
270 **FIG. 3.** Geometry of the NP-COM-NP system for the transmission coefficient calculation.

272 that the system has metallic properties and can conduct DC or AC current (see Figs. 1 and 2).

273 To confirm the NP-COM-NP system static conductivity, the transmission coefficient $T(E)$, i.e., the probability that an electron with energy E injected at one electrode will be transmitted to the other one, was calculated in the frame of Landauer methodology using the method of Non-Equilibrium Green Functions (NEGF), which was first proposed in 1960s by Keldysh and others^{44,45} and is widely used now.⁴⁶ The $T(E)$ function of the polyacetylene chain $\text{C}_8\text{H}_8\text{S}_2$ connected to two gold electrodes via the sulfur atoms was calculated (see Fig. 3) using the OpenMX package.⁴⁷ The length of the $\text{C}_8\text{H}_8\text{S}_2$ chain was equal to 11.6 Å. Semi-infinite one-dimensional gold nanorods with a pentagonal section of ~ 5 Å radius were considered as electrodes. $T(E)$ was calculated with zero potential bias at the electrodes (see Fig. 4). The resulting $T(E)$ function at a low voltage is obtained as ≈ 1 , which confirms that the electron can easily transfer from one NP to the other.

288 IV. PLASMON CALCULATION MODEL

289 To build the plasmon model, it is desirable to construct a differential equation of harmonic oscillations, such as in the model for bulk plasmons (1). However, while in the latter case the source of the



293 **FIG. 4.** Transmission coefficient spectrum (in units of $2 \times 10^2/h$) of the NP-COM-NP system. The energy is measured with respect to the Fermi level of the leads.

restoring force is the homogeneous polarization and surface charge density, in NP-COM systems, the restoring force arises due to the electric field between the two nanoparticles having opposite charges and due to the electrochemical potential μ difference of the nanoparticles. In the proposed hybrid model, it is desirable to use the results of calculations of conductive properties of the NP-COM-NP systems on the basis of the parameters derived from quantum-chemical calculations. Furthermore, the existence of a few number of quantum conductive channels in COM and a huge number of electronic states in the vicinity of E_{Fermi} of NPs must be taken into account.

The model is based on the assumption that the total energy of the NP-COM-NP system is constant so that

$$\frac{dE_{tot}}{dt} = \frac{d(E_{tot1} + E_{tot2} + E_{tot3})}{dt} = 0, \quad (5)$$

where $E_{tot1}, E_{tot2}, E_{tot3}$ are the total energies of the first and the second nanoparticles and the bridge molecule between them, respectively. These energies can be changed with charge variation in time $E_{tot_i} = E_{tot_i}(Q_i(t))$, where $i = 1 \dots 3$. We also assume that the charge distribution inside both nanoparticles correspond to the ground states, so from (5) follows

$$\frac{dE_{tot_i}}{dt} = \frac{dE_{tot_i}}{dQ_i} \frac{dQ_i}{dt} \quad i = 1 \dots 2. \quad (6)$$

Geometry optimization end calculations of electronic properties of a family consisting of six icosahedron shaped similar gold nanoparticles consisting of 55, 147, 309, 561, 923, and 1415 atoms (see Fig. 5) were carried out by the DFTB method⁴² with use of a parameter set that is appropriate for the description of bulk gold clusters and bulk material, as well as Au_nSCH_3 clusters.⁵³ A calculation of the band structure for the periodical structure $-[Au_{147}SC_8H_8S]-$ was also made. Furthermore, for using in (6) the total energies E_{tot} of the isolated gold nanoparticles having different total charges, $Q(e) \in \{-2, -1, 0, 1, 2\}$ were calculated (Table I).

It was found that the total energy of the all considered nanoparticles is well approximated by the quadratic function of the charge (Fig. 6), i.e.,

$$E_{tot} = aQ^2 + bQ + c. \quad (7)$$

The coefficients of determination R^2 in all cases were higher than 0.9999. In these quadratic functions, the coefficient c is the total energy, and the coefficient b is the opposite value of the Fermi energy of the corresponding neutral nanoparticle correspondingly (see Tables I and II). According to the well-known formula of the charged sphere electrostatic energy [$E = Q^2/(2C)$], the coefficient a

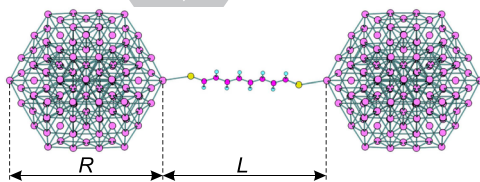


FIG. 5. Geometry of the $Au_{147}-S-C_8H_8-S-Au_{147}$ system.

TABLE I. Total energies E_{tot} and Fermi levels E_f of neutral and charged gold nanoparticles (everything is in a.u.).

Q	Au ₅₅		Au ₁₄₇		Au ₃₀₉	
	E_{tot}	E_f	E_{tot}	E_f	E_{tot}	E_f
2	-156.810	-0.384	-420.710	-0.313	-885.377	-0.293
1	-157.149	-0.294	-420.988	-0.249	-885.644	-0.243
0	-157.399	-0.204	-421.201	-0.184	-885.861	-0.193
-1	-157.559	-0.113	-421.351	-0.120	-886.029	-0.143
-2	-157.630	-0.022	-421.436	-0.056	-886.147	-0.093

Q	Au ₅₆₁		Au ₉₂₃		Au ₁₄₁₅	
	E_{tot}	E_f	E_{tot}	E_f	E_{tot}	E_f
2	-1608.594	-0.276	-2647.436	-0.260	-4059.262	-0.252
1	-1608.851	-0.235	-2647.677	-0.225	-4059.498	-0.222
0	-1609.066	-0.194	-2647.884	-0.191	-4059.705	-0.192
-1	-1609.241	-0.153	-2648.056	-0.156	-4059.883	-0.163
-2	-1609.374	-0.113	-2648.194	-0.122	-4060.030	-0.133

makes it possible to determine the capacities C of the considered Au clusters as $C = 1/(2a)$.

In Fig. 7, the dependence of the capacitance C for gold nanoparticles on their radius is shown. It is obvious that this dependence is linear. Since it is not clear how to define the radius of a nanoparticle, two dependencies are presented—on the maximal r_{max} and on the minimal r_{min} radius (Table II). The first one is taken as a distance to the atom at the cluster vertex; the second is a distance from the cluster central atom to the cluster faces. The coefficients of R^2 were in both cases were higher than 0.9998. The linear coefficients of the straight lines (1.13 and 0.84) in Fig. 7 show in both cases that for some average radius $R_{aver} \in [r_{min} \dots r_{max}]$ of the particle, its capacitance will coincide with the results of the classical electrostatics $C = R$, i.e., the capacitance of the nanoparticle is equivalent to that of a conducting sphere and equal to the average nanoparticle radius R_{aver} . We speculate that the existence of free terms in both linear dependencies, which do not change much, is related to the bulk distribution of the extra charge inside the particle. In any case, this contribution is significantly smaller than the surface

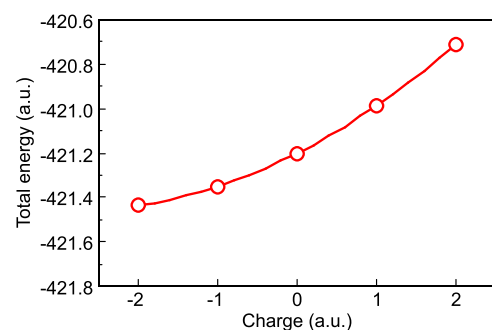


FIG. 6. Dependence of the Au_{147} nanoparticle total energy on the charge.

384 **TABLE II.** Coefficients of the quadratic dependence $E = f(Q)$ and nanoparticles radii
385 (everything is in a.u.).
386

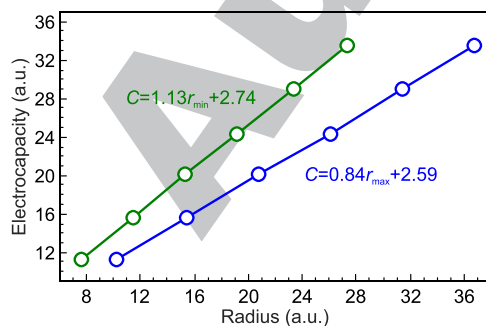
387 Cluster	a	b	c	r_{\max}	r_{\min}
388 Au ₅₅	0.0447	0.205	-157.399	7.55	10.17
389 Au ₁₄₇	0.0320	0.182	-421.201	11.41	15.49
390 Au ₃₀₉	0.0249	0.193	-885.861	15.33	20.81
391 Au ₅₆₁	0.0206	0.195	-1609.066	19.18	26.12
392 Au ₉₂₃	0.0172	0.190	-2647.884	23.42	31.43
393 Au ₁₄₁₅	0.0149	0.192	-4059.705	27.36	36.78

395 contribution, which suggests that additional charge is almost completely
396 distributed over the nanoparticle surface.
397

398 Equation (7) also assumes that extra-charge in the particle is distributed
399 according to the ground state. Actually, the relaxation of nonequilibrium
400 electrons occurs with a frequency $\nu \approx \tau^{-1}$, where τ^{-1} is the reciprocal
401 time between electron collisions. For small nanoparticles, this time is even
402 reduced due to the scattering at the nanoparticle boundaries. For gold, $\tau \sim 29$
403 fs⁵⁶ and we assume that the frequency of the plasmons under consideration
404 is much less than this inverse value; hence, the nanoparticles having a
405 varying charge can be considered to be in the ground state under the
406 plasmon oscillations.

407 The dependency of the total energy of the two isolated nanoparticles
408 with index i $E_{tot_i}(Q_i)$ was calculated as described in Sec. III [see
409 (7)], where b_i denote the nanoparticle chemical potentials. Using the
410 fact that the volumes of both nanoparticles are much larger than the
411 volume of the conductive molecule, most likely the electronic density of
412 the states (DOS) at the Fermi level E_f for the two nanoparticles
413 $DOS(E_f)_{NP_1}$ and $DOS(E_f)_{NP_2} \gg DOS(E_f)_{COM}$. It means that
414 with the change of E_f , the change of cluster charges follow
415 ΔQ_{NP_1} and $\Delta Q_{NP_2} \gg \Delta Q_{COM}$, and that during the plasmon
416 oscillations, the charges $Q_i(t)$ of both nanoparticles are opposite,
417 and the conducting molecule would stay neutral. Following this situation
418 and assuming that the two nanoparticles are identical, one gets

$$419 \frac{d(E_{tot_1} + E_{tot_2})}{dt} = [(b_1 - b_2) + (a_1 + a_2)2Q_1] \frac{dQ_1}{dt}, \quad (8)$$



421 **FIG. 7.** Dependence of the Au nanoparticles capacitance on their radius.

422 where $Q_1 = Q_1(t)$ is the charge of the first nanoparticle. Furthermore,
423 by the virtue of the argument stated above, this charge of the nanoparticle
424 will be denoted $Q(t)$, and the derivative $\frac{dQ_1(t)}{dt}$ will be denoted as a
425 current,
426

$$427 \frac{dQ_1(t)}{dt} \equiv I(t). \quad (9)$$

428 This implies that the electron freely moves from one particle through the
429 conducting molecule to the other particle. In reality, it is necessary to take
430 into account and determine the transmission probability T as the probability
431 for an electron to transmit through the bridge multiplied by the number of
432 transverse modes, each of which transfers electron through the bridge. Using
433 the definition data, the total energy of the two isolated nanoparticles in (8)
434 can be rewritten as

$$435 \frac{d(E_{tot_1} + E_{tot_2})}{dt} = 4aQ(t)I(t). \quad (10)$$

436 Unfortunately, in (5)–(10), it was assumed the two nanoparticles do not
437 influence each other. In contrast, due to the electrostatic interaction their
438 total energy is rewritten as

$$439 \frac{dE_{tot_{1-2}}}{dt} = 4aQ(t)I(t) - \frac{d}{dt} \left[F(R, L) \frac{Q(t)^2}{2R + L} \right] \\ 440 = Q(t)I(t) \left(4a - 2 \frac{F(R, L)}{2R + L} \right), \quad (11)$$

441 where the second term on the right side equation corresponds to the
442 derivative of the electrostatic interaction of the two opposite charges
443 at a distance $2R + L$ between the NP centers. A correction function
444 $F(R, L)$ is introduced to take into account the difference between the
445 interaction of the two conducting spheres (nanoparticles) and point
446 charges at the polarized spheres. The function $F(R, L)$ was addressed
447 in Refs. 57 and 58, where it was shown that this function decreases
448 rapidly from 2.0 when two conducted spheres are touching to 1.0
449 when $\frac{L}{2R} \rightarrow \infty$ and $F(R, L) \simeq 1.07$ at $\frac{L}{2R} = 1.4$.⁵⁸ Next, the force
450 acting on the conduction electron (hole) inside the conducting molecule
451 is obtained as

$$452 F(x, t) = -eE(x, t) - e[\vec{v}\vec{B}], \\ 453 E(x, t) = -\nabla\phi(x, t) - \frac{\partial A}{\partial t}. \quad (12)$$

454 We recall that for one-dimensional carriers moving in the COM, the
455 Lorentz magnetic force in the second right term of (12) should be
456 neglected.

457 Assuming that the characteristic size \tilde{R} of the system is much smaller
458 than the wavelength of the electromagnetic wave or $\tilde{R} \ll cT$, where the
459 T is the period of EMF and c is the light velocity, the quasistatic
460 approximation (QSA) may be used in the model. It means that EMF
461 delay effects can be neglected. In QSA, the characteristic speed of
462 electrons are much smaller than c ($v \ll c$), and the bias current
463 is much smaller than the conduction current: $|\frac{\partial D}{\partial t}| \ll |j|$
464 in QSA $\Delta\Delta(\vec{x}, t) = -\frac{4\pi}{c}I(x, t)$, where $I(x, t)$ is the current at
465 coordinate x passing through the COM at the time t . By estimation,
466 taking into account the speed of light in the atomic system of units
467 $C \simeq 137$ and the magnitude of the current $I(x, t) \approx \frac{e}{L}v_{Fermi}$, the

second term in the right part of (12) can be neglected and the force acting on the carriers can be defined as the gradient of the electrostatic potential $\nabla\phi(x, t)$ only. Furthermore, in QSA, the current reads

$$j = \sigma E, \text{div}(j) \approx 0, \quad (13)$$

and so it is possible to disregard the inhomogeneity of the current inside the conductive molecule and $I(x, t) = I(t)$.

Opposite to the Landauer approach, where the free electron or hole dynamics inside the COM of NP-COM-NP system under EMF is not analyzed, we have to do just that for building the plasmon differential equation. As it was mentioned above, it is assumed that this carrier dynamics is similar to the dynamics in periodical (NP-COM) systems under the same EMF. Assuming that the EMF is sufficiently small for Zener or avalanche breakdown, the electrons (holes) will be accelerated according to the effective mass tensor near the Fermi level. Due to the 1D nature of the carrier movement, this tensor transforms to the carrier effective mass value

$$m^* = \hbar^2 \left[\frac{d^2 E}{dk^2} \right]_{k=k_f}^{-1}. \quad (14)$$

In the following, we will build our model in relation to the periodic $[\text{Au}_{147}\text{-S-C}_8\text{H}_8\text{-S}]$ system. According to Fig. 2, the system is metallic. The calculated effective mass value $m^* = -0.454 m_e$ was calculated for the system using (14). Due to the system symmetry and the symmetry ($k \Rightarrow -k$), the total current of the free electrons and holes near E_{fermi} is cancelled without any AC electromagnetic field. In other words, the linear dependence of energy $E(k)$ is insignificant and the parabolic dependence

$$E(k) = \frac{(\hbar k)^2}{2m^*} \quad (15)$$

should be used for the carriers. We recall that the COM stays neutral under plasmon generation; hence, the total number of carriers inside the COM does not change under an applied weak EMF. The COM total energy E_{tot3} can be written via a sum of electrons in the conduction band, having different quasimomentum (15),

$$E_{tot3} = \sum_i n_i \frac{\hbar^2 k_i^2}{2m^*},$$

where n_i -occupation degrees of electrons having quasimomentum k_i .

Taking into account that under the influence of a weak electric field, the carriers are excited only near the Fermi level, we can write the energy derivative

$$\frac{dE_{tot3}}{dt} = n_f \frac{\hbar k}{m^*} \left[\frac{d(\hbar k)}{dt} \right]_{k=k_f}, \quad (16)$$

where n_f -occupation degrees of electrons having Fermi quasimomentum $k = k_f$. Due to spin degeneracy and generation of holes with the same effective mass upon excitation of electrons near the Fermi level, in the future, we will consider only electrons for which $n_f = 4$.

Following Ref. 43 and Eqs. (2), (3), and (15), the current and its derivative can be expressed as

$$I(t) = \frac{-en_f}{L} \frac{1}{\hbar} \frac{\partial E(k)}{\partial k} = \frac{-en_f}{L} \frac{\hbar k}{m^*} \Big|_{k=k_f}, \quad (17)$$

$$\frac{dI(t)}{dt} = \frac{-en_f}{Lm^*} \frac{d(\hbar k)}{dt} \Big|_{k=k_f}, \quad (18)$$

where L is the length of COM.

Combining (16)–(18), the E_{tot3} derivative is equal to

$$\frac{dE_{tot3}}{dt} = I(t) \frac{dI(t)}{dt} \frac{m^* L^2}{ne^2}. \quad (19)$$

Using (9), (11), and (19), Eq. (5) is transformed into

$$\frac{dE_{tot}}{dt} = Q(t)I(t) \left(4a - 2 \frac{F(R, L)}{2R + L} \right) + I(t) \frac{d^2 Q(t)}{dt^2} \frac{m^* L^2}{ne^2} = 0. \quad (20)$$

Dividing by $I(t)$, one can get a differential equation of the harmonic oscillations having the square of modified plasmonic frequency $\widetilde{\omega}_{pl}^2$,

$$\frac{d^2 Q(t)}{dt^2} = -\widetilde{\omega}_{pl}^2 Q(t), \quad (21)$$

$$\widetilde{\omega}_{pl}^2 = \left(\frac{1}{C} - \frac{F(R, L)}{2R + L} \right) \frac{2ne^2}{m^* L^2}. \quad (22)$$

Here, substitution $C = 1/(2a)$ is used again. From this equation, one can see that the square of modified plasmonic frequency $\widetilde{\omega}_{pl}^2$ is similar with expression of conventional plasma frequency $\omega_{pl}^2 = 4\pi ne^2/(m^* \Omega)$, where n denotes the number of electrons occupying the volume Ω . Under the assumption of $R \gg L$, remembering that $C \approx R$ (NP radius) and replacing the expression in parentheses of (22) by $1/R$, one gets

$$\widetilde{\omega}_{pl}^2 \approx \frac{2ne^2}{m^* L^2 R} = \frac{4\pi ne^2}{m^* \widetilde{\Omega}}, \quad (23)$$

where $\widetilde{\Omega} = 2\pi RL^2$ —effective volume per n electrons. Comparing $\widetilde{\omega}_{pl}^2$ and ω_{pl}^2 , we can verify that the modified plasma frequency resides in the infrared (IR) region. For example, in the bulk gold, one electron has a volume of 16.85 \AA^3 , and the plasmonic frequency ω_{pl} is $\approx 9.1 \text{ eV}$. Using the parameters of the investigated system containing the nanoparticle of 147 gold atoms ($(R) \approx 14.0 \text{ \AA}$, $L \approx 14.3 \text{ \AA}$), the estimation of the modified plasma frequency is $\widetilde{\omega}_{pl} \approx 0.35 \text{ eV}$.

In order to show the influence of system geometric parameters (R, L) on the plasmon frequency, we plotted $\widetilde{\omega}_{pl}$ as a function of the nanoparticle radius R for three conducting molecules $[\text{-S-C}_n\text{H}_n\text{-S}]$ ($n = 6, 7, 8$), having different length L (see Fig. 8 and legend there). The electron effective mass was here taken again as $m^* = 0.454 m_e$.

One can see that in the proposed NP-COM-NP systems, the plasmonic frequencies are expected to lie in the IR region and are very significantly changed with a change of the system geometric parameters.

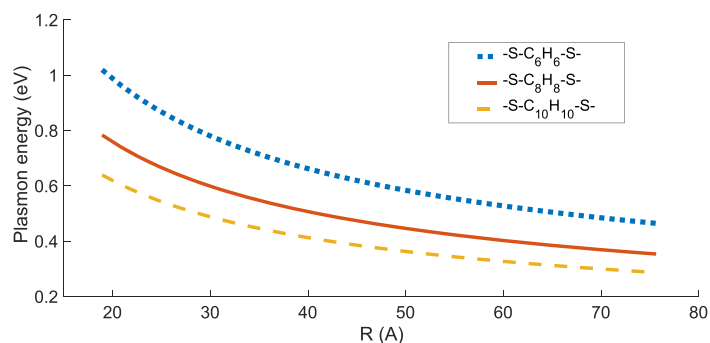


FIG. 8. The dependence of plasmon frequency of nanoparticle on its radius R for three conducting molecules $-\text{[S-C}_n\text{H}_n\text{-S]}-$ ($n = 6, 7, 8$).

V. CONCLUSION

In this work, the possibility of generating specific plasmons due to charge transfer in a couple of metal nanoparticles bridged by conductive molecules is investigated. To describe the properties of such plasmons, an original quantum-classical model was developed based on a description of the time dependence of the ballistic current through the conductive bridge and which includes quantum effects. For the test system, consisting of two gold nanoparticles bridged by the conjugated polyacetylene molecule C_8H_8 terminated by sulfur atoms, an analytical expression for the frequency of the plasmons was derived. Our approach can be qualified from the fact that although approaches based on calculations of nonequilibrium Green functions or real-time propagation of wave functions in principle can be applied to describe ballistic transport, their complexity disallows the description of real sophisticated systems of the kind considered here. The model proposed in this work resolves this problem since it uses only band structure information that can be easily obtained from the calculations of the corresponding periodic system, whose unit cell consists of the connected nanoparticle and the conductive molecule. It was shown that for the systems under study, the plasmon frequency is determined by expression (23), which is similar to the one for bulk materials. Herewith, the effective density of the conduction electrons becomes, in the present case, significantly lower than the density of conduction electrons in the bulk material. It results in shifting the modified plasmon frequency to the IR region. The strong dependence of the modified plasmon frequency on the system conductivity makes it possible to use such NP-COM-NP systems to build different chemical sensors which can be based on a change in the conductivity of the conducting molecule during its chemical interaction with external molecules. Such an interaction can thus significantly change the conjugated character of the π -bonding in the molecule and, therefore, its conductivity. The conductivity directly changes the effective mass and, according to (22), the plasmon frequency, that can be easily measured. We believe that this new type of plasmon can have an unprecedented impact on the field of deep tissue chemical sensing.

ACKNOWLEDGMENTS

This study was supported by the Russian Science Foundation, Project No. 18-13-00363.

REFERENCES

- 1 A. Uddin and X. Yang, *J. Nanosci. Nanotechnol.* **14**, 1099 (2014).
- 2 J. Liu, H. He, D. Xiao, S. Yin, W. Ji, S. Jiang, D. Luo, B. Wang, and Y. Liu, *Materials* **11**, 1833 (2018).
- 3 J. Olson, S. Dominguez-Medina, A. Hoggard, L.-Y. Wang, W.-S. Chang, and S. Link, *Chem. Soc. Rev.* **44**, 40 (2015).
- 4 L. Guo, J. A. Jackman, H.-H. Yang, P. Chen, N.-J. Cho, and D.-H. Kim, *Nano Today* **10**, 213 (2015).
- 5 A. N. Koya and J. Lin, *Appl. Phys. Rev.* **4**, 021104 (2017).
- 6 N. Elahi, M. Kamali, and M. H. Baghersad, *Talanta* **184**, 537 (2018).
- 7 Z. Farka, T. Juřík, D. Kovář, L. Trnková, and P. Skládal, *Chem. Rev.* **117**, 9973 (2017).
- 8 K. A. Willets, A. J. Wilson, V. Sundaresan, and P. B. Joshi, *Chem. Rev.* **117**, 7538 (2017).
- 9 C. Deeb and J.-L. Pelouard, *Phys. Chem. Chem. Phys.* **19**, 29731 (2017).
- 10 S. Linic, U. Aslam, C. Boerigter, and M. Morabito, *Nat. Mater.* **14**, 567 (2015).
- 11 M. Valenti, M. P. Jonsson, G. Biskos, A. Schmidt-Ott, and W. A. Smith, *J. Mater. Chem. A* **4**, 17891 (2016).
- 12 A. E. Ershov, V. S. Gerasimov, A. P. Gavriluk, S. V. Karpov, V. I. Zakomirnyi, I. L. Rasskazov, and S. P. Polyutov, *J. Quant. Spectrosc. Radiat. Transfer* **191**, 1–6 (2017).
- 13 I. L. Rasskazov, S. V. Karpov, and V. A. Markel, *Opt. Lett.* **38**(22), 4743–4746 (2013).
- 14 I. L. Rasskazov, S. V. Karpov, G. Y. Panasyuk, and V. A. Markel, *J. Appl. Phys.* **119**(4), 043101 (2016).
- 15 V. I. Zakomirnyi, I. L. Rasskazov, V. S. Gerasimov, A. E. Ershov, S. P. Polyutov, S. V. Karpov, and H. Ågren, *Photonics Nanostruct. - Fundam. Appl.* **30**, 50–56 (2018).
- 16 V. I. Zakomirnyi, I. L. Rasskazov, S. V. Karpov, and S. P. Polyutov, *J. Quant. Spectrosc. Radiat. Transfer* **187**, 54–61 (2017).
- 17 V. I. Zakomirnyi, I. L. Rasskazov, V. S. Gerasimov, A. E. Ershov, S. P. Polyutov, and S. V. Karpov, *Appl. Phys. Lett.* **111**(12), 123107 (2017).
- 18 N. Venugopal, A. E. Gerasimov, V. S. Ershov, S. V. Karpov, and S. P. Polyutov, *Opt. Mater.* **72**, 397–402 (2017).
- 19 F. Parveen, B. Sannakki, M. V. Mandke, and H. M. Pathan, *Sol. Energy Mater. Sol. Cells* **144**, 371 (2016).
- 20 S. Gwo, H.-Y. Chen, M.-H. Lin, L. Sun, and X. Li, *Chem. Soc. Rev.* **45**, 5672 (2016).
- 21 K. Ueno, T. Oshikiri, Q. Sun, X. Shi, and H. Misawa, *Chem. Rev.* **118**, 2955 (2018).
- 22 M. Ujihara, *J. Oleo Sci.* **67**, 689 (2018).
- 23 S. Lee and I. Choi, *Biochip J.* **13**, 30 (2019).
- 24 A. Crut, P. Maioli, F. Vallée, and N. D. Fatti, *J. Phys.: Condens. Matter* **29**, 123002 (2017).
- 25 R. Esteban, A. G. Borisov, P. Nordlander, and J. Aizpurua, *Nat. Commun.* **3**, 825 (2012).

- 636 ²⁶R. Esteban, A. Zugarramurdi, P. Zhang, P. Nordlander, F. J. Garcia-Vidal, A. G.
637 Borisov, and J. Aizpurua, *Faraday Discuss.* **178**, 151 (2015).
638 ²⁷W. Zhu, R. Esteban, A. G. Borisov, J. J. Baumberg, P. Nordlander, H. J. Lezec,
639 J. Aizpurua, and K. B. Crozier, *Nat. Commun.* **7**, 11495 (2016).
640 ²⁸P. Hohenberg and W. Kohn, *Phys. Rev.* **136**, B864 (1964).
641 ²⁹W. Kohn and L. J. Sham, *Phys. Rev.* **140**, A1133 (1965).
642 ³⁰E. Runge and E. K. U. Gross, *Phys. Rev. Lett.* **52**, 997 (1984).
643 ³¹X. L. Lozano, C. Mottet, and H.-Ch. Weissker, *J. Phys. Chem. C* **117**, 3062
(2013).
644 ³²V. Kulkarni, E. Prodan, and P. Nordlander, *Nano Lett.* **13**, 5873 (2013).
645 ³³E. Townsend and G. W. Bryant, *Nano Lett.* **12**, 429 (2012).
646 ³⁴X. López-Lozano, H. Barron, C. Mottet, and H.-C. Weissker, *Phys. Chem.*
647 *Chem. Phys.* **16**, 1820 (2014).
648 ³⁵V. Kulkarni and A. Manjavacas, *ACS Photonics* **2**, 987 (2015).
649 ³⁶J. M. Ziman, *Electrons and Phonons: The Theory of Transport Phenomena in*
650 *Solids* (Oxford University Press, New York, 1960).
651 ³⁷A. Varas, P. García-González, J. Feist, F. J. García-Vidal, and A. Rubio,
652 *J. Nanophotonics* **5**, 409 (2016).
653 ³⁸X. López-Lozano, H. Barron, C. Mottet, and H.-C. Weissker, *Phys. Chem.*
654 *Chem. Phys.* **16**, 1820 (2014).
655 ³⁹G. Kresse and J. Furthmüller, *Comput. Mater. Sci.* **6**, 15 (1996).
656 ⁴⁰G. Kresse and J. Furthmüller, *Phys. Rev. B* **54**, 11169 (1996).
657 ⁴¹M. Sukharev and M. Galperin, *Phys. Rev. B* **81**, 165307 (2010).
⁴²R. Landauer, *Philos. Mag.* **21**, 863 (1970). 658
⁴³S. Datta, *Quantum Transport: Atom to Transistor* (Cambridge University Press,
659 New York, 2005). 660
⁴⁴L. V. Keldysh, *JETP* **20**, 1018 (1965). 661
⁴⁵L. P. Kadanoff and G. Baym, *Quantum Statistical Mechanics*, *Frontiers in*
662 *Physics Lecture Notes* (Benjamin; Cummings, 1962). 663
⁴⁶G. Stefanuci and R. van Leewuen, *Non-Equilibrium Many-Body Theory of*
664 *Quantum Systems* (Cambridge, 2013). 665
⁴⁷See www.openmx-square.org for ■. 666
⁴⁸U. Peskin, *Fortschr. Phys.* **65**, 1600048 (2017). 667
⁴⁹M. Sukharev and M. Galperin, *Phys. Rev. B* **81**, 165307 (2010). 668
⁵⁰A. J. White, M. Sukharev, and M. Galperin, *Phys. Rev. B* **86**, 205324 (2012). 669
⁵¹M. Kuperman and U. Peskin, *Molecular Electronics: A Theoretical and Experi-*
670 *mental Approach* (Taylor & Francis, 2015). 671
⁵²B. Aradi, B. Hourahine, and T. Frauenheim, *J. Phys. Chem. A* **111**, 5678 (2007). 672
⁵³A. Fihey, C. Hettich, J. Touzeau, F. Maurel, A. Perrier, C. Köhler, B. Aradi, and
673 T. Frauenheim, *J. Comput. Chem.* **36**, 2075 (2015). 674
⁵⁴F. Alkan and C. M. Aikens, *J. Phys. Chem. C* **122**, 23639 (2018). 675
⁵⁵N. V. Ilawe, M. B. Oviedo, and B. M. Wong, *J. Mater. Chem. C* **6**, 5857 (2018). 676
⁵⁶P. B. Johnson and R. W. Christy, *Phys. Rev. B* **6**, 4370 (1972). 677
⁵⁷W. R. Smythe, *Static and Dynamic Electricity* (McGraw-Hill Book Company,
678 Inc., 1950). 679
⁵⁸V. A. Saranin, *Phys. - Usp.* **42**, 385 (1999). 680